

4d resonant inelastic x-ray scattering in gadolinium

J.-J. Gallet, J.-M. Mariot, and C. F. Hague

*Laboratoire de Chimie Physique-Matière et Rayonnement (CNRS associate), Université Pierre et Marie Curie,
11 rue Pierre et Marie Curie, F-75231 Paris Cedex 05, France*

F. Sirotti

*Laboratoire pour l'Utilisation du Rayonnement Electromagnétique (CEA, CNRS, MENESR), Campus Universitaire d'Orsay,
Bâtiment 209D, F-91405 Orsay Cedex, France*

M. Nakazawa, H. Ogasawara, and A. Kotani

Institute for Solid State Physics, University of Tokyo, Roppongi, Minato-ku, Tokyo 106, Japan

(Received 12 August 1996)

Resonant inelastic x-ray scattering (RIXS) involving selective excitations to Gd $4d^9 5p^6 4f^{n+1}$ intermediate states has been measured. An x-ray resonant Raman effect is clearly identified for excitation to states below the $4d$ ionization threshold. RIXS spectra have been calculated for several excitation energies and provide a good quantitative explanation for the large variation in the $5p \rightarrow 4d$ branching ratio intensities observed as a function of excitation energy. Weak structure observed close to the elastic peak is identified as the result of spin-flip scattering. [S0163-1829(96)51044-1]

The availability of high flux x-ray synchrotron radiation and new efficient instrumentation has recently stimulated widespread interest in resonant inelastic x-ray scattering (RIXS).¹⁻³ The RIXS process, also known as x-ray resonant Raman scattering, is an x-ray absorption (photon energy ω_1) followed by x-ray emission (photon energy ω_2) in which a bound electron is promoted to an empty state and the core hole left behind decays via the radiative transfer of a less bound electron.

Excitations involving the $2p$ core levels of rare earths fall into a relatively favorable energy region (5–8 keV) for several synchrotron radiation sources. This explains that some of the more important RIXS experiments recently performed have been concerned with these thresholds. The experiments of Hämäläinen *et al.*⁴ and Krisch *et al.*⁵ are worthy of special mention. The former measured the Dy $2p_{3/2}$ absorption edge by monitoring the x-ray fluorescence in a fixed narrow energy band as primary photon energies were scanned across the edge. New structure in the absorption spectra was attributed to the elimination of the core level lifetime broadening. These experiments have since been reinterpreted by Tanaka *et al.*⁶ and Carra *et al.*⁷ The RIXS experiments by Krisch *et al.*⁵ address the problem of separating contributions to the white line in the Gd $2p_{3/2}$ absorption from quadrupolar ($2p \rightarrow 4f$) and dipolar ($2p \rightarrow 5d$) transitions. They cannot be separated using x-ray-absorption spectroscopy (XAS) because of core-hole lifetime broadening.

The $4d$ x-ray emission spectra of the rare earths were first studied in detail by Zimkina and co-workers⁸⁻¹⁰ using electron beam excitation. Based on their work on all the lanthanides, they suggested an interpretation of the complex $4d$ emission spectra in terms of three types of transitions: $5p \rightarrow 4d$, $4d^9 4f^{n+1} \rightarrow 4d^{10} 4f^n$, and $4d^9 4f^n \rightarrow 4d^{10} 4f^{n-1}$. Only recently has selective photon excitation been used to excite the $4d \rightarrow 4f$ resonances in BaF₂.¹¹ Other experiments involving the La and Ba $5p \rightarrow 4d$ spectra obtained with a

polychromatic photon excitation have also been discussed recently.¹²

Here we report on RIXS involving the excitation of the Gd metal $4d$ core electrons into $4f$ states. We find that apart from the $4d^9 4f^{n+1} \rightarrow 4d^{10} 4f^n$ recombination process, the decay of the $4d$ hole is dominated by the $5p \rightarrow 4d$ channel, i.e., the intermediate state $|i\rangle$ which has the $4d^9 5p^6 4f^{n+1}$ configuration decays to $4d^{10} 5p^5 4f^{n+1}$. It should be noted that in earlier experiments with electron beam excitation the $3d \rightarrow 4f$ recombination peak was called a resonance line because it coincides in energy with a white line in the XAS spectrum.¹³ The cross section for such a process is large enough to be observed even with polychromatic excitation, such as electron beam excitation, because of the high degree of localization of $4f$ electrons. In an x-ray-scattering experiment, this is an elastic process which will therefore coincide with other elastically scattered radiation.

Resonant excitation along with calculated spectra now make it possible to reliably identify most of the structure. It should also be noted that the resonant excitations studied here are to states below the photoionization threshold as opposed to the $4d \rightarrow 4f$ resonances studied in a $4f$ compound (BaF₂) by Rubensson *et al.*¹¹

The experiments were performed on undulator beamline SU7 at Super ACO. The 20-pole undulator feeds a 10-m toroidal grating monochromator. The energy resolution of the latter was set to 0.6 eV for the RIXS experiments. The energy distribution of the scattered x rays was measured with a grating spectrometer fitted to the existing end station (ABS6) equipped with an electron energy analyzer and evaporation sources. The x-ray spectrometer is based on Nordgren's design.¹⁴ A two-dimensional position sensitive detector was used to record the spectra. The resolution was set to ≈ 0.4 eV. For constructional reasons the angle between the incoming photon beam and the direction of observed scattered radiation was 45°. Thus, although the sample was

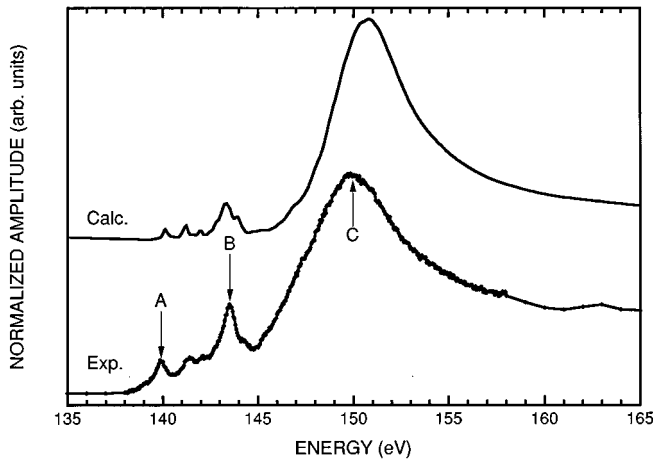


FIG. 1. Gd $4d$ absorption spectrum: (a) Experiment. (b) Theoretical prediction. Arrows A, B, and C indicate the incoming photon energies used in the x-ray inelastic scattering calculations.

mounted for p polarization, elastic scattering was not minimized. The elastic peak served to calibrate the x-ray-emission energy scale.

The sample was prepared *in situ* by electron bombardment. The base pressure was 7×10^{-11} mbar with a brief rise to the 10^{-9} mbar range at the start of evaporation. Gadolinium was deposited onto a silicon wafer to a total thickness of ≈ 700 Å, ensuring that the recorded spectra were those of the metal. A small contribution from the oxide is certainly not ruled out but valence-band photoelectron spectra also confirmed that sample contamination was low. The $4d$ XAS spectrum (Fig. 1) was recorded by measuring the photocurrent.

RIXS measurements performed for the typical incoming photon energies labeled A, B, and C in Fig. 1 are plotted in Fig. 2. For clarity, the spectra are normalized to the same amplitude in the 100–130 eV energy region. The elastic peak reaches its maximum amplitude at 150 eV. At the other ex-

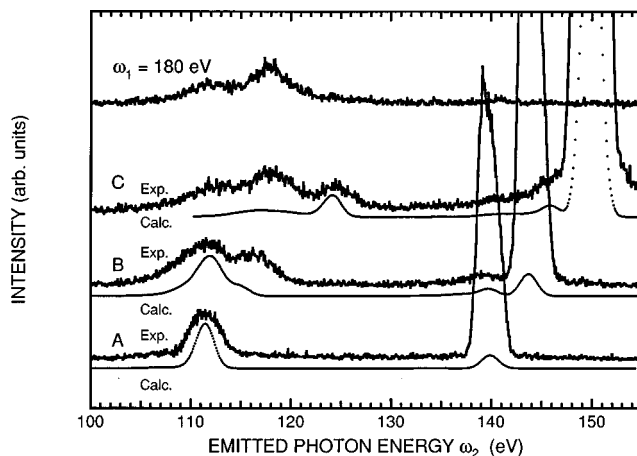


FIG. 2. Gd resonant inelastic x-ray-scattering spectrum in the vicinity of the $4d$ ionization threshold: observed (raw data) and calculated (smooth curve) for energies A, B, and C (see Fig. 1).

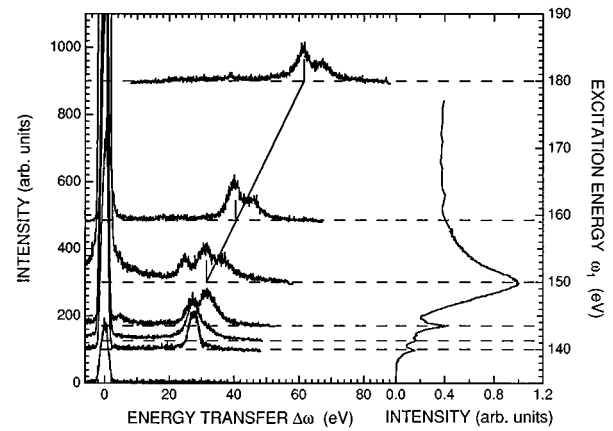


FIG. 3. Gd resonant inelastic x-ray-scattering spectrum plotted as a function of the energy transfer. The line indicates the contribution of the normal x-ray emission to the process, i.e., ω_2 independent of ω_1 .

citation energies we used, its amplitude drops by a factor of 10. This indicates that the $4d \rightarrow 4f$ absorption process followed by $4f \rightarrow 4d$ x-ray emission has a strong probability when the excitation is set to above the ionization threshold.

Where excitation is to the multiplets below the ionization threshold, the spectra reflect the energy transfer $\Delta\omega = \omega_1 - \omega_2$ corresponding to the electronic excitation from $5p$ to $4f$. It is therefore instructive to plot the spectra on a transfer energy scale. This is done in Fig. 3 for values of ω_1 from 135 to 180 eV and in Fig. 4 for five values of ω_1 below the ionization threshold. We note that when the excitation energy is kept below the ionization threshold the energy transferred is constantly ≈ 27 eV for values of ω_1 close to A in the absorption spectrum. It unambiguously indicates a resonant x-ray Raman process. Similarly, a peak at ≈ 25 eV

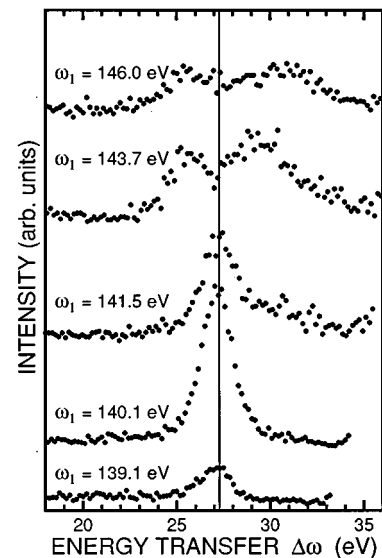


FIG. 4. Detail of resonant Raman effect for excitations close to A and B (see Fig. 1).

observed for excitations close to peak *B*. Above the ionization threshold, the spectrum moves away from the elastic peak as the energy of the photon increases. This is the footprint of normal x-ray fluorescence, i.e., the usual $5p_{3/2} \rightarrow 4d$ and $5p_{1/2} \rightarrow 4d$ spin-orbit split doublet. (To be more exact, the Coulomb and exchange interactions in the $5p^5 4f^7$ configuration also give some minor contribution to this doublet structure.)

The calculations for Gd $4d$ XAS and RIXS have been performed for a Gd^{3+} free ion taken as a good approximation to Gd metal. The multiplet coupling originating from the Coulomb and exchange interactions and the spin-orbit interaction is fully taken into account using Cowan's atomic structure code.¹⁵ The Slater integrals, F^k and G^k , and the spin-orbit coupling constants, ζ_{4d} and ζ_{4f} , are calculated by the Hartree-Fock program with relativistic correction. Then the values of $F^k(4f,4f)$, $F^k(4d,4f)$, and $G^k(4d,4f)$ are reduced to 80%, 75%, and 66% of the Hartree-Fock values, respectively. The values of $F^k(5p,4f)$ and $G^k(5p,4f)$ are reduced to 80% of the Hartree-Fock values.

The calculation of Gd $4d$ XAS has been made in just the same way as by Ogasawara and Kotani,¹⁶ where they took into account the interference effect (Fano effect) between $4d \rightarrow 4f$ and $4f \rightarrow \epsilon g$ transitions through the $4d-4f4f$ super Coster-Kronig transition. For details on the calculation see Ref. 16. The calculated result is shown in Fig. 1. Agreement with experiment is good with the prethreshold peaks *A* and *B* and the giant band *C* clearly identified. The prethreshold peaks are dipole forbidden transitions, in the *LS*-coupling scheme, from the Hund's rule ground state 8S , the *LS* terms of the final states of *A* and *B* being 8D and 6D , respectively. They become weakly allowed due to the spin-orbit interaction. On the other hand, the giant band is dipole allowed with an 8P final state.

Using the Kramers-Heisenberg formula which describes a coherent second-order optical process, and keeping only the resonant term, the RIXS spectrum is represented by

$$F(\omega_1, \omega_2) = \sum_f \left| \left\langle f \left| \left(V_R \frac{1}{E_g + \omega_1 - H - V_A + i\gamma} V_R \right) \right| g \right\rangle \right|^2 \times \delta(E_g + \omega_1 - E_f - \omega_2), \quad (1)$$

where $|g\rangle$ and $|f\rangle$ are ground and final states with energies E_g and E_f , respectively. The operator V_R represents the dipole transitions of the $4d \rightarrow 4f$, $4f \rightarrow \epsilon g$, $4d \rightarrow 5p$, and their inverse processes. The operator V_A represents the Coster-Kronig transition, the Hamiltonian H describes the atomic electronic states, and γ is taken as $\gamma \rightarrow +0$. The calculated result for Gd RIXS is shown in Fig. 2 for incident photon energies *A*, *B*, and *C*.

In our calculation of RIXS, we assume that the incident photon is unpolarized, for simplicity. When the incident photon energy tuned to the prethreshold peak *A*, the RIXS shows a single peak at $\omega_2 = \omega_1$. We also find a double peak structure near $\omega_2 \approx 111.5$ eV and 107 eV, where the lower-energy peak is visible only on an expanded scale. The peak at $\omega_2 = \omega_1$ corresponds to the elastic scattering, where the x-ray emission occurs by the $4f \rightarrow 4d$ transition, resulting in the

8S final state, which is the same as the ground state. On the other hand, the doublet structure is caused by the $5p \rightarrow 4d$ transition corresponding to the final states with a hole in the $5p_{3/2}$ and $5p_{1/2}$ states. The branching ratio of the doublet structure depends strongly on the intermediate state, and in the case of *A* the lower energy peak ($5p_{1/2}$ hole) is weak, as already mentioned. This result is in agreement with experimental data. When ω_1 is tuned to *B* in the calculation, we have a weak inelastic scattering peak (a satellite to the elastic peak) about 4 eV to the lower-energy side of the elastic scattering peak. A similar structure is also observed experimentally. This satellite peak originates from the spin-flip scattering due to the $4f \rightarrow 4d$ dipole transition, where the final state is 6P corresponding to the spin flip from the 8S ground state. Furthermore, the branching ratio of the doublet structure is inverted in going from *A* to *B*, which fits excellently experimental observation. A similar change of the branching ratio of the $5p$ spin-orbit split final states has also been observed in the resonant photoemission of La.¹⁷

When ω_1 is tuned to the energy of the giant absorption band *C*, we also have a weak spin-flip satellite in the $4f \rightarrow 4d$ transition, and the higher-energy peak of the $5p$ doublet structure again becomes stronger than the lower-energy one as for excitation to *A*. The experimental data for *C* shows a three peak structure instead of the $5p$ spin-orbit doublet. This difference between the calculated and experimental results can be explained by an additional x-ray-emission process, which is not taken into account in our theory. It is well known that the excited state of the giant band can be autoionized, i.e., an excited $4f$ electron is transferred to the continuum state ϵf . We would expect x-ray emission occurring after this autoionization to produce additional structure whose spectral shape and energy position would be similar to those of the normal x-ray fluorescence corresponding to the case where ω_1 is much higher than the $4d$ excitation threshold (or the giant band). We have taken into account neither the autoionization process nor the normal x-ray emission in our calculation, but we note that the experimental result of the normal x-ray emission exhibits a double-peak structure (see Fig. 2 for $\omega_1 = 180$ eV). Therefore, if we superpose the normal x-ray emission and the calculated RIXS for *C* with an appropriate intensity ratio, it is possible to reproduce the three-peak structure. The position of the lower-energy peak of RIXS almost coincides with the higher-energy peak of the normal x-ray emission, which results in the middle peak of the three-peak structure.

In summary, we have shown that selective excitation of $4d$ electrons to 8D and 6D prepeaks in the absorption curve lead to a resonant x-ray Raman effect in Gd where the $4d^9 5p^6 4f^{n+1}$ intermediate state decays to a $4d^{10} 5p^5 4f^{n+1}$ final state. This incidentally gives access to the $5p^5 4f^{n+1}$ configuration, which is normally dipole forbidden starting from the $4d^{10} 5p^6 4f^n$ ground-state configuration. Considerable variations are observed in the $5p_{3/2,1/2} \rightarrow 4d$ branching ratio. The calculation excellently reproduces this effect and shows that the branching ratio depends critically on the intermediate state. Other interesting inelastic scattering effects of weak intensity, observed experimentally, are identified as the consequence of spin-flip scattering resulting from the $4d \rightarrow 4f$ excitation.

- ¹Y. Ma, Phys. Rev. B **49**, 5799 (1994).
- ²Y. Ma, K. E. Miyano, P. L. Cowan, Y. Aglitzkiy, and B. A. Karlin, Phys. Rev. Lett. **74**, 478 (1995).
- ³J. A. Carlisle, E. L. Shirley, E. A. Hudson, L. J. Terminello, T. A. Callcott, J. J. Jia, D. L. Ederer, R. C. C. Perera, and F. J. Himpsel, Phys. Rev. Lett. **74**, 1234 (1995).
- ⁴K. Hämäläinen, D. P. Siddons, J. B. Hastings, and L. E. Berman, Phys. Rev. Lett. **67**, 2850 (1991).
- ⁵M. H. Krisch, C. C. Kao, F. Sette, W. A. Caliebe, K. Hämäläinen, and J. B. Hastings, Phys. Rev. Lett. **74**, 4931 (1995).
- ⁶S. Tanaka, K. Okada, and A. Kotani, J. Phys. Soc. Jpn. **63**, 2780 (1994).
- ⁷P. Carra, M. Fabrizio, and B. T. Thole, Phys. Rev. Lett. **74**, 3700 (1995).
- ⁸V. A. Fomichev, S. A. Gribovskii, and T. M. Zimkina, Fiz. Tverd. Tela (Leningrad) **15**, 201 (1973) [Sov. Phys. Solid State **15**, 138 (1973)].
- ⁹S. A. Gribovskii and T. M. Zimkina, Fiz. Tverd. Tela (Leningrad) **15**, 300 (1973) [Sov. Phys. Solid State **15**, 217 (1973)].
- ¹⁰S. A. Gribovskii, V. A. Fomichev, and T. M. Zimkina, Fiz. Tverd. Tela (Leningrad) **15**, 1312 (1973) [Sov. Phys. Solid State **15**, 894 (1973)].
- ¹¹J.-E. Rubensson, J. Lüning, S. Eisebitt, and W. Eberhardt, Phys. Rev. B **51**, 13 856 (1995).
- ¹²D. R. Mueller, J. S. Wallace, J. J. Jia, W. L. O'Brien, Q.-Y. Dong, T. A. Calcott, K. E. Miyano, and D. L. Ederer, Phys. Rev. B **52**, 9702 (1995).
- ¹³C. Bonnelle and R. C. Karnatak, C. R. Acad. Sci. B **268**, 494 (1969); J. Phys. (France) **32 C4**, 230 (1971).
- ¹⁴J. Nordgren, G. Bray, S. Cramm, R. Nyholm, J.-E. Rubensson, and N. Wassdahl, Rev. Sci. Instrum. **60**, 1690 (1989).
- ¹⁵R. D. Cowan, *The Theory of Atomic Structure and Spectra* (University of California Press, Berkeley, 1981).
- ¹⁶H. Ogasawara and A. Kotani, J. Phys. Soc. Jpn. **64**, 1394 (1995).
- ¹⁷H. Ogasawara, A. Kotani, B. T. Thole, K. Ichikawa, O. Aita, and M. Kamada, Solid State Commun. **81**, 645 (1992).